ISSN 1392–1320 MATERIALS SCIENCE (MEDŽIAGOTYRA). Vol. 25, No. 1. 2019

Dependence of Electrical and Optical Properties of Sol-gel-derived SnO_2 Thin Films on Sb-substitution

Elisée MUHIRE [1], Jiao YANG [2], Xuejian HUO [1], Meizhen GAO [1]*

[1] *Key Lab for Magnetism and Magnetic Materials of Ministry of Education, School of Physical Science and Technology, Lanzhou University, Lanzhou 730000, China*
[2] *School of Physics and Engineering, Henan University of Science and Technology, Henan 471003, China*

crossref http://dx.doi.org/10.5755/j01.ms.25.1.19172

Received 30 September 2017; accepted 29 January 2018

In the present work, Sb-doped SnO_2 (ATO) thin films were deposited on Si substrates by spin-coating method and the influence of Sb-doping on surface roughness, structural, optical and electrical properties has been investigated. AFM measurements show that the surface roughness decreases with increasing the Sb-doping concentration up to 5 mol%. XRD results confirm that all prepared ATO films have a tetragonal rutile structure of tin oxide. It has been observed that both the crystallite size and the extinction coefficient decrease with increasing Sb-doping concentration up to 5 mol%, while the refractive index increases with increasing Sb-doping concentration. The electrical resistivity decreases with increasing Sb-doping concentration, and the lowest resistivity obtained is 8.5×10^{-3} Ω.cm for SnO_2 doped with 7.5 mol% of Sb.

Keywords: SnO_2 thin films, spin-coating, optical constants, resistivity.

1. INTRODUCTION

In recent years, tin oxide (SnO_2) thin films received much attention due to their combination of a wide band-gap energy of 3.6 eV at 300 K [1 – 4], unique electrical and optical properties. This allows SnO_2 thin films to be considered as important transparent conductive oxide (TCO) films with potential applications in optoelectronic devices [5 – 8], gas sensors [4, 5, 9], dye sensitized solar cells [10], and lithium-ion batteries [11, 12]. Undoped tin oxide possesses a low conductivity leading to high electrical resistivity and this prevents it from commercial applications [13]. To meet the market demands of SnO_2 thin films, a large variety of metals or ions can be doped into SnO_2 thin films to improve both optical and electrical properties [13 – 15]. Among different dopants, antimony (Sb) appears to be a suitable dopant for SnO_2 since the substitution of Sn^{4+} by Sb^{5+} into SnO_2 lattice highly improves the n-type semiconductor characteristics of SnO_2 [14, 16]. Furthermore, antimony doped tin oxide (ATO) thin films are transparent conductive oxide (TCO) films seeing that they combine excellent electrical properties, high transparency in visible region and chemical stability [14, 17 – 19]. Therefore, it is very significant to prepare ATO thin films for a broad series of applications.

Currently, ATO thin films have been prepared by different methods including electro-deposition and dip-coating [20], sputtering techniques [13, 16, 21], spray ultrasonic method [14, 22], chemical spray pyrolysis technique [23, 24], sol-gel techniques [15, 19, 25, 26], plasma-assisted molecular epitaxy [27]. Compared with other preparation methods, herein, ATO thin films were prepared by sol-gel spin-coating method due to its simplicity, low cost and high effectiveness.

Although there are many research works on physical characterization of ATO thin films, few studies focused on the correlation between Sb doping concentration, resistivity and optical constants of ATO thin films prepared by sol-gel technique. Herein, the optical constants like refractive index and extinction coefficient of ATO films were obtained after model fit of spectroscopic ellipsometry data by using a uniaxial model fit, which has not yet been explored in previous works.

The spectroscopic ellipsometry measurements were performed over a spectrum range of 400-1700 nm and yielded the experimental ellipsometric parameters Ψ and Δ, from which the optical constants and film thicknesses were extracted after a model fit. The refractive index of ATO thin films was found to increase with a corresponding increase in Sb-doping concentration while the extinction coefficient decreased.

2. EXPERIMENTAL DETAILS

2.1. Materials

$SnCl_4 \cdot 5H_2O \geq 99.0$ % and $SbCl_3 \geq 99$ % were supplied by Sinopharm Chemical Reagent Co., Ltd; 2-methoxyethanol and ethanolamine were supplied by Tianjin Kaixin Chemical Industry co. LTD. All chemicals were directly used without further purification.

2.2. Sample preparation

ATO thin films were prepared according to the following procedure; 5 mmol of $SnCl_4 \cdot 5H_2O$ were dissolved in 30 mL of 2-methoxyethanol and then calculated amount of $SbCl_3$ at a molar ratio varying from 0 to 7.5 mol% were added, followed by addition of few drops of ethanolamine used as a stabilizing agent. The mixture solution was refluxed at 80 °C for 4 hours and after that the obtained suspension was aged for 36 hours to

* Corresponding author. Tel.: +86-13639335271; fax: +86-931-8913554.
E-mail address: *gaomz@lzu.edu.cn* (M.Z. Gao)

ensure its stability and viscosity. ATO films were fabricated on silicon substrates using spin-coating method. The substrates were pre-cleaned by sonication in acetone, isopropanol and in methanol solvents for 10 minutes each, rinsed in deionized water and then dried in an oven at 100 °C for 30 minutes. The solutions were deposited on substrates at a rotating speed of 3000 rpm for 30 sec. After each coating-layer, the films were dried on a hot-plate at 300 °C for 10 minutes to remove the organic residuals and allow the evaporation of the solvent; the coating and drying were repeated for 9 times to obtain the needed thickness. Finally, undoped and Sb-doped SnO_2 thin films were annealed in a tube furnace at 500 °C for 1 hour to improve their crystallinity.

2.3. Characterization

The surface roughness was measured by Atomic Force Microscope (AFM) technique performed on an Asylum Research MFP-3D in a tapping mode, and the film thickness was determined by both scanning electron microscope (SEM) and spectroscopic ellipsometry (SE) measurements. The crystal structure and phase identification were determined by X-ray diffraction (XRD) measurements performed on Philips X'PertPro with Cu Kα radiation (λ = 1.5418 Å) at a scan rate of 0.03 °/min within 2θ angle ranging between 20° – 80°. The elemental composition and bond states of the films were analyzed by multifunctional X-Ray Photoelectron Spectroscopy (XPS) Kratos AXIS Ultra^{DLD}. Spectroscopic ellipsometry measurements were performed for all prepared ATO thin films by Woollam Variable Angle Spectroscopic Ellipsometer (WVASE 32) over a spectral region ranging between 400 – 1700 nm in a step of 10 nm at two different angles of incidence of 65° and 75° with a step of 10° in order to evaluate the optical constants of the films.

3. RESULTS AND DISCUSSION

3.1. Surface roughness and film thickness

The surface roughness is a key factor to be investigated since it provides a clue about the quality of the optical material under study [28]. From AFM three-dimensional images of Fig. 1, the surface roughness decreases from 0.59 nm for undoped SnO_2 to 0.48, 0.11 and 0.35 nm for ATO film with 2.5, 5.0 and 7.5 mol% of Sb. The ATO film with 5 mol% of Sb doping holds the lowest surface roughness, which is in good agreement with the variation of the crystallite size.

Fig. 2 shows the SEM cross-sectional images for undoped and Sb-doped tin oxide films. The film thickness is found to decrease from 196.1 nm for undoped SnO_2 to 180.4 nm, 178.0 nm and 151.8 nm for ATO with 2.5, 5.0 and 7.5 mol% of Sb; respectively. The difference between the film thicknesses determined from SEM cross-sectional images and those obtained from spectroscopic ellipsometry measurements is trivial and is shown in Table 1.

3.2. Phase and crystallite size analysis

Fig. 3 shows the XRD patterns of the as-prepared ATO thin films, clarifying that the (110), (101), (200), (211), (220), (310) and (301) diffraction peaks are assigned to the tetragonal rutile structure of SnO_2, (JCPDS Card No 41-1445), with some silicon standard peaks detected from the substrate which are marked with a star in Fig. 3.

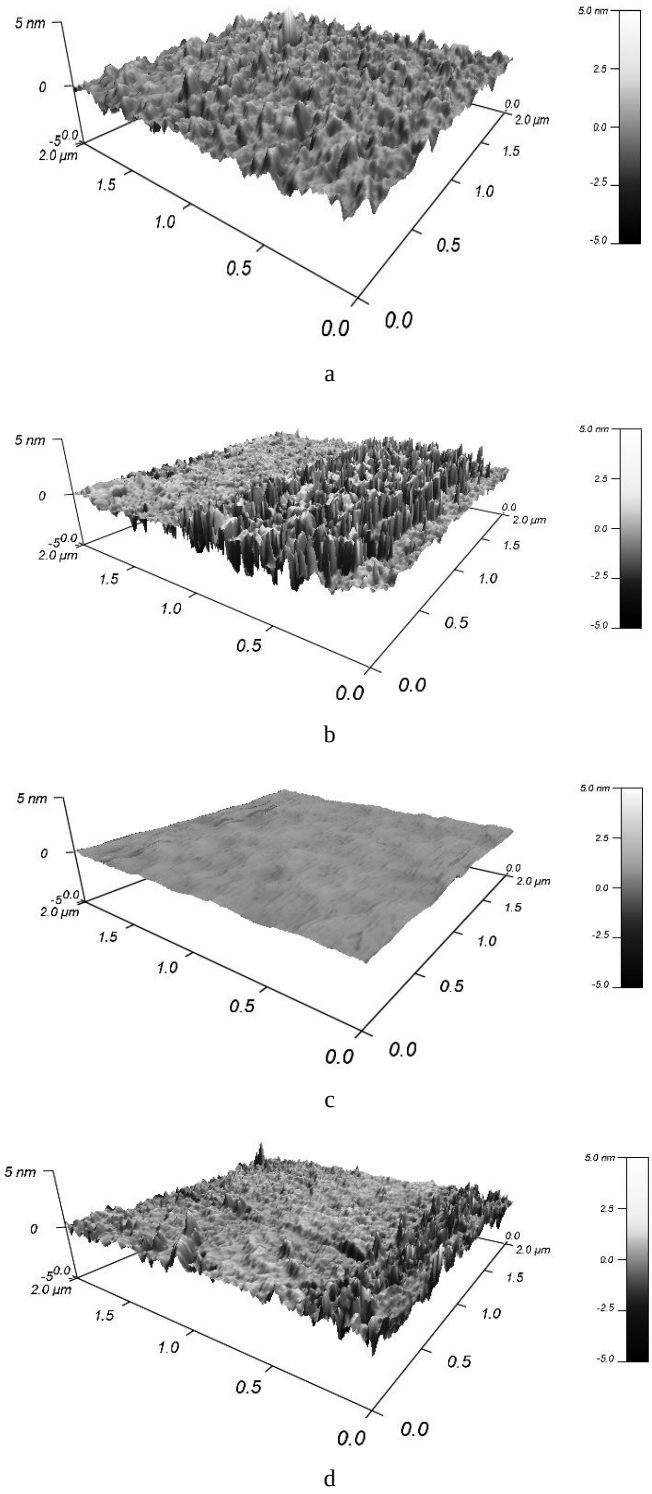

Fig. 1. AFM 3D images of the as-prepared ATO thin films with different Sb-doping concentration a – 0 mol% Sb; b – 2.5 mol% Sb; c – 5.0 mol% Sb; d – 7.5 mol% Sb annealed at 500 °C for 1 h

Interestingly, the peak corresponding to (110) reflection is found to be the preferred orientation for the as-prepared ATO films and this is in consistence with literature [13, 26, 29, 30].

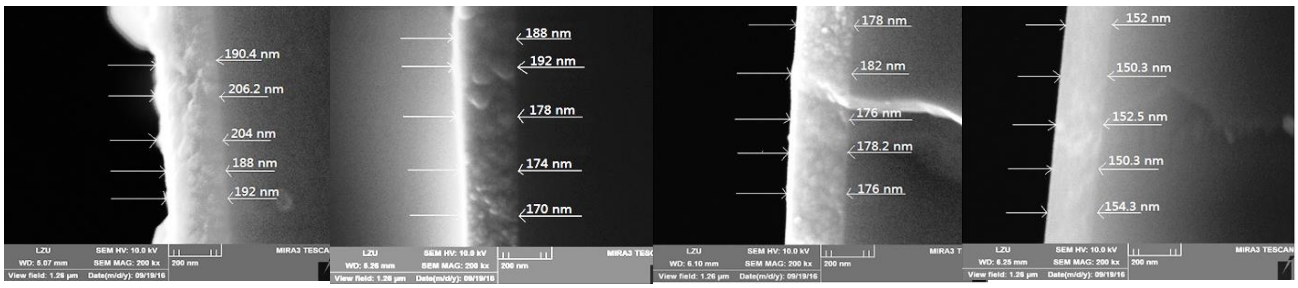

a b c d

Fig. 2. SEM cross-sectional images: a – SnO_2; b – ATO-2.5; c – ATO-5.0; d – ATO-7.5

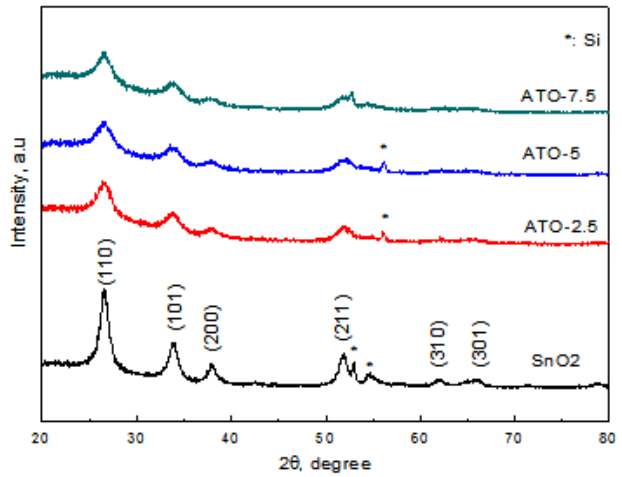

Fig. 3. XRD patterns of the as-prepared ATO films with different Sb-doping concentrations, all films were annealed at 500 °C for 1 h

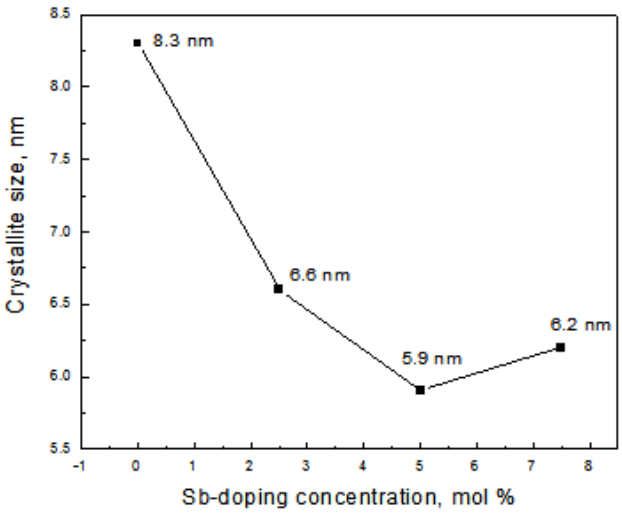

Fig. 4. Variation of the crystallite size of ATO thin films as a function of Sb-doping concentration

It can be clearly observed that after Sb incorporation, some weak diffraction peaks disappear and others become wider and their intensities become lower due to grain size reduction and lattice distortion confirming the incorporation of Sb^{5+} into SnO_2 lattice. Fig. 4 shows the variation of the crystallite size estimated from XRD data using MDI Jade software. The crystallite size decreases from 8.3 nm for undoped SnO_2 to 6.6, 5.9 nm for ATO with 2.5, 5.0 mol% of Sb, respectively as illustrated in Fig. 4. However, when the doping concentration increases to 7.5 mol%, a small increase (0.3 nm) in crystallite size is observed compared to 5 mol%.

By considering the obtained AFM results and the estimated crystallite sizes, we can conclude that the optimum Sb-doping concentration is 5 mol%. The doped Sb could substitute Sn in ATO film efficiently up to 5 mol% concentration. When the doping concentration greater than 5 mol%, the extra Sb appears as impurity, and when the doping concentration is lower than 5 mol%, less Sn^{4+} could be substituted by Sb^{5+}. Therefore, the ATO film with 5 mol% of Sb exhibits lower surface roughness and smaller crystallite size.

3.3. Chemical composition analysis

Fig. 5 a shows the XPS survey spectra of both undoped and Sb-doped SnO_2 films, which illustrates the presence of Sn, Sb and O in all ATO thin films. As shown in high magnification XPS spectra of Sn 3d (Fig. 5 b), the binding energies of $Sn3d_{5/2}$ and $Sn3d_{3/2}$ are found at around 486.6 eV and 495.1 eV, respectively; and the separation between their binding energies is equal to 8.5 eV, which confirms the presence of Sn^{4+} in all as-prepared thin films [17, 31].

The detailed XPS spectra of Sb 3d and O 1s (Fig. 5 c) confirms the existence of Sb 3d in ATO thin films, where the binding energies of Sb $3d_{5/2}$ and Sb $3d_{3/2}$ are located at 531.0 eV and 540.1 eV, respectively.

From Fig. 5 c, the peak at a binding energy of 530 – 532 eV shows that Sb 3d5/2 and O 1s overlap, which is in consistence with the literature [4, 32 – 35]. The deconvolution XPS peak of Sb $3d_{3/2}$ is shown in Fig. 5 d and confirms the coexistence of Sb^{5+} and Sb^{3+} into SnO_2 lattice sites [15, 17, 32, 35] with Sb^{3+} located on the surface and grain boundaries of ATO films [4, 21, 33]. The high percentage of Sb^{5+} contributes to an increase of carrier concentration, therefore a decrease in resistivity of ATO films [30].

3.4. Optical studies

3.4.1. Spectroscopic ellipsometry measurements

Spectroscopic Ellipsometry (SE) is a suitable non-destructive technique to analyze the thickness and optical constants (refractive index and the extinction coefficient) of thin films [35 – 37].

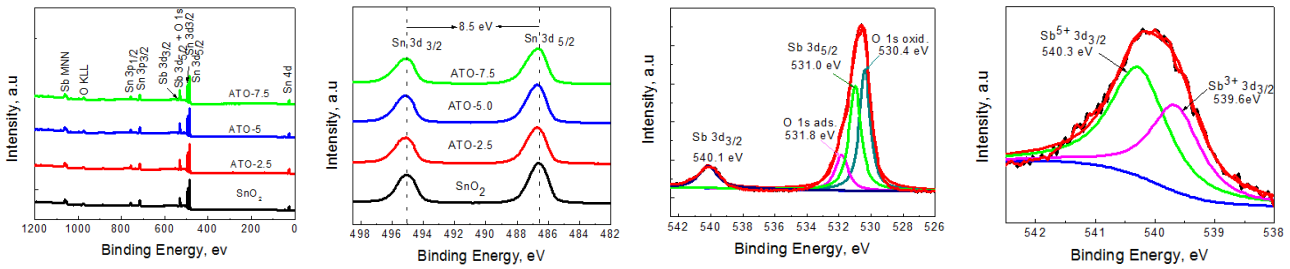

a b c d

Fig. 5. XPS results of the as-prepared ATO thin films annealed at 500 °C for 1 h: a – survey spectra of all ATO thin films with different Sb-doping concentrations; b – high magnification XPS spectra of Sn 3d for all samples; c – high magnification of O 1s+Sb $3d_{5/2}$; d – the deconvolution spectra of Sb $3d_{3/2}$ for ATO-7.5

The ellipsometric measurements actually yield the ellipsometric parameters Ψ and Δ, which are then simulated using an adequate model fit to extract the optical constants and film thickness [35, 38]. The ellipsometric parameters Ψ and Δ are most often related using the equation [35, 37]

$$\rho = \frac{R_p}{R_s} = \tan\psi \exp(i\Delta), \quad (1)$$

where R_p and R_s are the complex reflection coefficients for light polarized parallel and perpendicular to the plane of incidence, respectively; $\tan\psi$ is the ratio of the amplitude reflection coefficients and Δ is the phase difference between p- and s- polarized waves [35]. To simultaneously determine the optical constants and the film thickness, a uniaxial anisotropic model was built for good fitting of ellipsometric experimental data. To model the ellipsometric data, a Cauchy-Urbach model was first built. After fitting all parameters, some misfits between generated and experimental data were obtained due to thickness non-uniformity. This may be caused by the sol-gel technique, which produces ATO films with uneven and inhomogeneous surfaces. Therefore, a non-uniformity and a uniaxial anisotropy were added to Cauchy-Urbach model. After fitting the parameters from the built model, an appropriate fit between ellipsometric generated and experimental data was obtained accompanied with an improved and acceptable mean-square error (MSE) representing the sum of squares of the differences between generated and experimental data as shown in Table 1; and the final model structure possesses three phases of a uniaxial anisotropic layer describing ATO, the 2.0 nm native oxide of silicon (SiO_2) layer and the Si substrate layer as illustrated in inset of Fig. 8, Fig. 6 and Fig. 7 illustrate the best fit between the generated and experimental ellipsometric parameters Ψ and Δ in a wavelength range of 400 – 1700 nm, respectively. After fitting the ellipsometric parameters Ψ and Δ, the determined film thickness was found to decrease with increasing Sb-doping concentration. The thickness decreases from 203.6 nm for undoped SnO_2, to 180.6 nm, 164.5 nm and 152.0 nm for ATO films with 2.5, 5.0 and 7.5 mol% of Sb; respectively, and their comparison with thicknesses determined from SEM cross-section images together with the obtained acceptable mean-square error (MSE) are illustrated in Table 1.

Table 1. The values of thicknesses, MSE and resistivity

Sample	d (SEM), nm	d (SE), nm	MSE	Resistivity, Ω.cm
SnO_2	196.1	203.6	12.2	$2.6\pm0.01\times10^{-1}$
ATO-2.5	180.4	180.6	17.8	$1.6\pm0.01\times10^{-2}$
ATO-5.0	178.0	168.6	21.5	$1.3\pm0.01\times10^{-2}$
ATO-7.5	151.8	152.0	61.4	$8.5\pm0.01\times10^{-3}$

3.4.2. Determination of the optical constants of Sb-doped SnO_2

It is believed that the refractive index and extinction coefficient are important parameters to describe the optical performance of TCO films used in solar cells and other optoelectronic devices. Fig. 8 reveals a clear and distinctive increase in refractive index as the Sb-doping concentration increases in a wavelength range of 400-1700 nm, and the obtained values of n of the as-prepared ATO films annealed at 500 °C for 1 hour vary between 1.54 and 1.77.

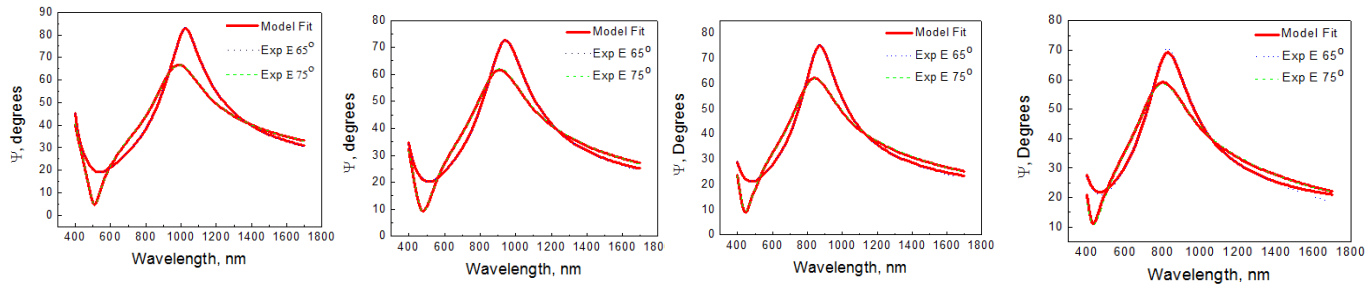

a b c d

Fig. 6. Measured and generated ellipsometric parameter Ψ of ATO thin films with variation of Sb concentration versus wavelength: a – SnO_2; b – ATO-2.5; c – ATO-5.0; d – ATO-7.5

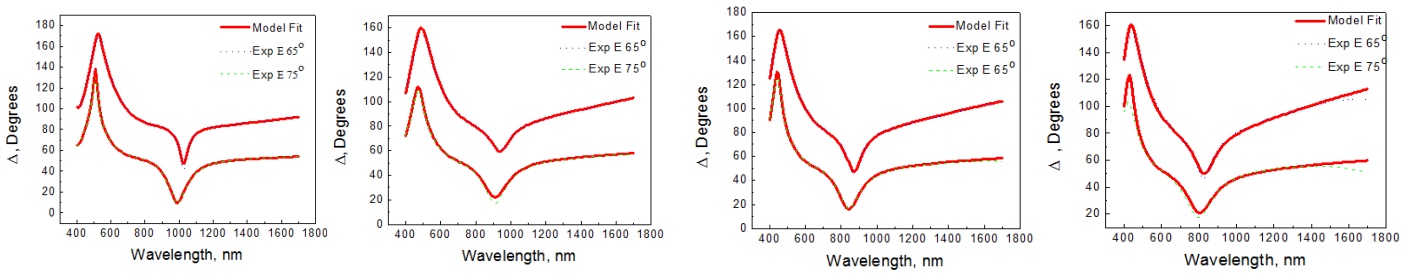

a b c d

Fig. 7. Measured and generated ellipsometric parameter *Δ* of ATO thin films with variation of Sb concentration versus wavelength: a – SnO_2; b – ATO-2.5; c – ATO-5.0; d-ATO-7.5

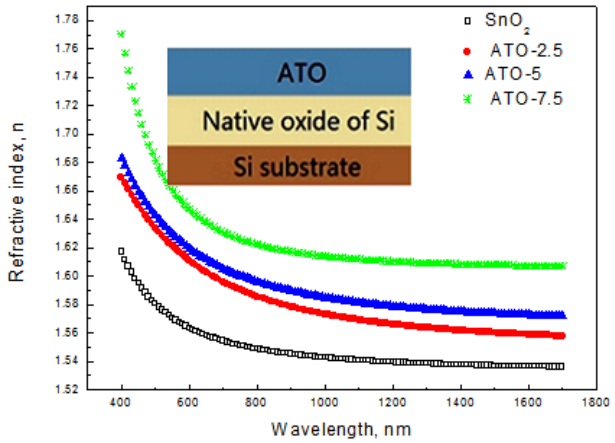

Fig. 8. Variation of the refractive index of undoped and Sb-doped SnO_2 thin films as a function of wavelength. The inset is the layered structure used to model the SE experimental data

Sibel et al. [14] also found the similar phenomenon of increasing refractive index in SnO_2:Sb after Sb incorporation; and Atay et al. [39] prepared SnO_2:F films exhibiting a little increase in values of refractive index of SnO_2:F with increasing F-doping concentration. The change in packing density of films to higher value with Sb incorporation into SnO_2 lattice, may lead to the increase in refractive index [40]. Fig. 9 shows the spectra of extinction coefficients extracted from fitted SE experimental data as a function of wavelength for different Sb-doping concentrations.

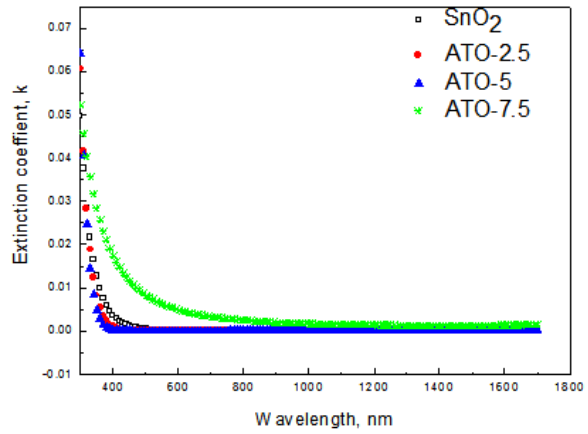

Fig. 9. Variation of the extinction coefficient of undoped and Sb-doped SnO_2 thin films as a function of wavelength ranging between 400 – 1700 nm

The extinction coefficients are extracted in a wavelength range between 400 – 1700 nm, in which the values of extinction coefficients are higher in short wave region and almost zero in visible and near-infrared region; which confirms that both undoped and Sb-doped SnO_2 thin films are transparent in this region. It is clearly seen that the extinction coefficient decreases with increasing Sb-doping concentration up to 5.0 mol% of Sb due to the decrease in crystallite size, whereas it increases for further increase of Sb-doping concentration to a molar ratio of 7.5 mol%, which is in good agreement with XRD results. This decrease in extinction coeffient of ATO films up to 5 mol% of Sb may be due to that the highest level of Sn^{4+} is substituted by Sb^{5+} and contributes the most electrons in ATO thin films with Sb-doping concentration of 5 mol%.

3.5. Electrical measurements

Fig. 10 illustrates the variation of the electrical resistivity of the films with dopant content, in which, after antimony incorporation into SnO_2 lattice, the resistivity decreases from 2.6×10^{-1} Ω.cm for undoped SnO_2 to 1.6×10^{-2} Ω.cm, 1.3×10^{-2} Ω.cm and 8.5×10^{-3} Ω.cm for SnO_2 thin films doped with 2.5, 5.0 and 7.5 mol% of Sb, respectively. These results are in consistence with the literature that the substitution of Sn^{4+} by Sb^{5+} leads to a generation of conduction electrons and increase in number of donors facilitating the decrease in electrical resistivity [41, 42], and hence this can enhance the conductivity of the ATO films as well.

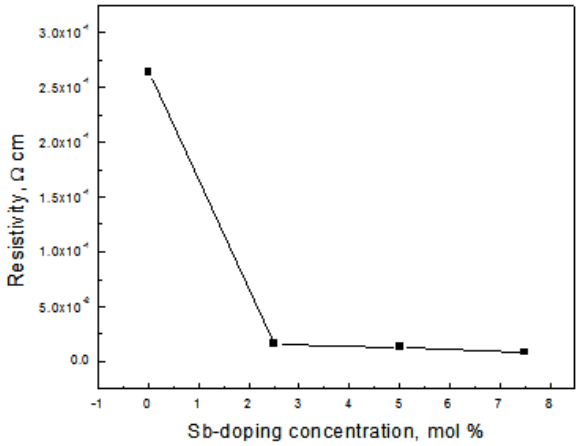

Fig. 10. Variation of resistivity of ATO thin films with Sb-doping concentration

4. CONCLUSIONS

Antimony doped tin oxide (ATO) thin films were prepared via sol-gel spin-coating method and effects of antimony-doping on optical constants, film thickness, resistivity and crystallite size of the ATO thin films are investigated. The surface roughness, extinction coefficient and crystallite size of ATO films decrease with increasing Sb-doping concentration up to 5.0 mol%, while the refractive index increases with increasing Sb. The electrical resistivity decreases with the increase in Sb-doping concentration, and the lowest resistivity obtained at room temperature is found to be 8.5×10^{-3} Ω.cm. By taking into account the obtained values of extinction coefficient and crystallite size together with the surface roughness, the optimum doping concentration for the present ATO films is 5 mol% of Sb.

Acknowledgments

The authors would like to express their gratitude to National Natural Science Foundation of China (51371093) for their invaluable support to this work.

REFERENCES

1. **Peiwei, H., Huaming, Y.** Controlled Coating of Antimony-doped Tin Oxide Nanoparticles on Kaolinite Particles *Applied Clay Science* 48 (3) 2010: pp. 368 – 374. https://doi.org/10.1016/j.clay.2010.01.008
2. **Wenfeng, M., Bangyun, X., Yong, L., Chunqing, H.** Correlation Between Defects and Conductivity of Sb-doped Tin Oxide Thin Films *Applied Physics Letters* 103 (3) 2013: pp. 031915. https://dx.doi.org/10.1063/1.4816084
3. **Abdullah, M.A.H., Mika, S., Tanujjal, B., Joydeep, D.** Efficient Photocatalytic Degradation of Phenol in Aqueous Solution by SnO_2:Sb Nanoparticles *Applied Surface Science* 370 2016: pp. 229 – 236. http://dx.doi.org/10.1016/j.apsusc.2016.02.123
4. **Szczuko, D., Werner, J., Oswald, S., Behr, G., Wetzig, K.** XPS Investigations of Surface Segregation of Doping Elements in SnO_2 *Applied Surface Science* 179 (1 – 4) 2001: pp. 301 – 306. https://doi.org/10.1016/S0169-4332(01)00298-7
5. **Marikkannan, M.,Vishnukanthan, V., Vijayshankar, A., Mayandi, J., Pearce, J.M.** A Novel Synthesis of Tin Oxide Thin Films by the Sol-gel Process for Optoelectronic Applications *American Institute of Physics Advances* 5 (2) 2015: pp. 027122. https://dx.doi.org/10.1063/1.4909542
6. **Mohamed, S.H.** SnO_2 Dendrites–nanowires for Optoelectronic and Gas Sensing Applications *Journal of Alloys and Compounds* 510 (1) 2012: pp. 119 – 124. https://doi.org/10.1016/j.jallcom.2011.09.006
7. **Tetsuo, T., Kato, F., Nakajima, T., Igarashi, K., Kumagaia, T.** Direct Conversion of Ametal Organic Compound to Epitaxial Sb-doped SnO_2 Film on a (0 0 1) TiO_2 Substrate using a KrF Laser, and its Tesulting Electrical Properties *Applied Surface Science* 255 (24) 2009: pp. 9808 – 9812. https://doi.org/10.1016/j.apsusc.2009.04.095
8. **Honglei, M., Honglei, M., Xiaotao, H., Jin, M., Ying-Ge, Y., Jie, H., De-heng, Z., Xian-Gang, X.** Thickness Deppendence of Properties of SnO_2:Sb Films Deposited on Flexible Substrates *Applied Surface Science* 191 (1 – 4) 2002: pp. 313 – 318. https://doi.org/10.1016/S0169-4332(02)00253-2
9. **Rameech, Mc.C., Nozomi, S., Umesh, S., Soumen, D., Amit, K., Hyoung, J.C., Ramki, K., Sudipta, S.** Laser Irradiated Nano-architectured Undoped Tin Oxide Arrays: Mechanism of Ultrasensitive Room Temperature Hydrogen Sensing *Nanoscale* 4 (22) 2012: pp. 7256 – 7265. https://dx.doi.org/10.1039/C2NR32217J
10. **Zhengdao, L., Yong, Z., Ruzhong, S., Yan, X., Haiquan, X., Zhigang, Z.** Nanostructured $Sn0_2$ photoanode–based dye–sensitized solar cells *Chinese Science Bulletin* 59 (18) 2014: pp. 2122 – 2134. https://doi.org/10.1007/s11434-013-0079-3
11. **Na, L., Huawei, S., Hao, C., Wang, C.l.** SnO_2 Nanoparticles Anchored on Vertically Aligned Graphene with a High Rate, High Capacity, and Long Life for Lithium Storage *Electrochimica Acta* 130 2014: pp. 670 – 678. https://dx.doi.org/10.1016/j.electacta.2014.03.081
12. **Qinqin, Z., Qinqin, Z., Lisha, M., Qiang, Z., Chenggang, W., Xu, X.** SnO_2-Based Nanomaterials: Synthesis and Application in Lithium-Ion Batteries and Supercapacitors *Journal of Nanomaterials* 2014: pp. 1 – 15. https://doi.org/10.1155/2015/850147
13. **Wenhao, Y., Shihui, Y., Yang, Z., Zhang, W.** Properties of Sb-doped SnO_2 Transparent Conductive Thin Films Deposited by Radio-frequency Magnetron Sputtering *Thin Solid Films* 542 2013: pp. 285 – 288. https://dx.doi.org/10.1016/j.tsf.2013.06.077
14. **Sibel, G., Tülay, S., Serin, N.** Studies on Optical Properties of Antimony Doped SnO_2 Films *Applied Surface Science* 352 2015: pp. 16 – 22. https://dx.doi.org/10.1016/j.apsusc.2015.03.057
15. **Wenfeng, M., Bangyun, X., Qichao, L., Yawei, Z., Chongshan, Y., Yong, L., He, C.** Influences of Defects and Sb Valence States on the Temperature Dependent Conductivity of Sb Doped SnO_2 Thin Films *Physics Letters A* 379 (36) 2015: pp. 1946 – 1950. https://dx.doi.org/10.1016/j.physleta.2015.06.033
16. **Bissig, B., Jäger, T., Ding, L., Tiwari, A.N., Romanyuk, Y.E.** Limits of Carrier Mobility in Sb-doped SnO_2 Conducting Films Deposited by Reactive Sputtering *Applied Physics Letters Materials* 3 2015: pp. 062802. https://dx.doi.org/10.1063/1.4916586
17. **Xu, J.M., Li, L., Wang, S., Ding, H.L., Zhang, Y.X., Li, G.H.** Influence of Sb Doping on the Structural and Optical Properties of Tin Oxide Nanocrystals *Crystal Engineering Communications* 15 2013: pp. 3296 – 3300. https://dx.doi.org/10.1039/C3CE40241J
18. **Rajpure, K.Y., Kusumade, M.N., Neumann-Spallart, N.M., Bhosale, C.H.** Effect of Sb Doping on Properties of Conductive Spray Deposited Sno_2 Thin Films *Materials Chemistry and Physics* 64 (3) 2000: pp. 184 – 188. https://doi.org/10.1016/S0254-0584(99)00256-4
19. **Mazloom, J., Ghodsi, F.E., Gholami, M.** Fiber-like Stripe ATO (Sno_2:Sb) Nanostructured Thin Films Grown by Sol – –gel Method: Optical, Topographical and Electrical Properties *Journal of Alloys and Compounds* 579 2013: pp. 384 – 393. https://dx.doi.org/10.1016/j.jallcom.2013.06.063
20. **Wang, Y., Fan, C.M., Hua, B., Liang, Z.H., Yan-Pin, S.** Photoelectrocatalytic Activity of Two Antimony Doped Sno_2 Films For Oxidation of Phenol Pollutants *Transaction*

of Nonferrous Metals Society of China 19 (3) 2009: pp. 778 – 783.
https://doi.org/10.1016/S1003-6326(08)60349-0

21. **Christoph, K., Péter, Á., Klein, A.** Surface and Bulk Properties of Sputter Deposited Undoped and Sb-doped Sno_2 Thin Films *Sensors and Actuators B* 139 (2) 2009: pp. 665 – 672.
https://doi.org/10.1016/j.snb.2009.03.067
22. **Achour, R., Atmane, B., Chaker, B., Boubaker, B., Gasmi, B.** Effect of Antimony Doping on the Structural, Optical and Electrical Properties of Sno_2 Thin Films Prepared by Spray Ultrasonic *Superlattices and Microstructures* 76 2014: pp. 105 – 114.
https://dx.doi.org/10.1016/j.spmi.2014.09.024
23. **Yadav, A.A.** Influence of Film Thickness on Structural, Optical, and Electrical Properties of Spray Deposited Antimony Doped Sno_2 Thin Films *Thin Solid Films* 591 2015: pp. 18 – 24.
https://dx.doi.org/10.1016/j.tsf.2015.08.013
24. **Esro, M., Georgakopoulos, S., Lu, H., Vourlias, G., Krier, A., Milne, W.I., Gillin, W.P., Adamopoulos, V.** Solution Processed SnO_2:Sb Transparent Conductive Oxide as an Alternative to Indium Tin Oxide for Applications in Organic Light Emitting Diodes *Journal of Materials Chemistry C* 4 2016: pp. 3563 – 3570.
https://dx.doi.org/10.1039/C5TC04117A
25. **Jing, K., Hongmei, D., Pingxiong, Y., Junhao, C.** Synthesis and Properties of Pure and Antimony-doped Tin Dioxide Thin Films Fabricated by Sol–gel Technique on Silicon Wafer *Materials Chemistry and Physics* 114 (2 – 3) 2009: pp. 854 – 859.
https://doi.org/10.1016/j.matchemphys.2008.10.049
26. **Giraldi, T.R., Escote, M.T., Bernardi, M.I.B., Bouquet, V., Leite, E.R., Longo, E., Varela, J.A.** Effect of Thickness on the Electrical and Optical Properties of Sb Doped SnO_2 (ATO) Thin Films *Journal of Electroceramics* 13 (1 – 3) 2004: pp. 159 – 165.
https://doi.org/10.1007/s10832-004-5093-z
27. **White, M.E., Bierwagen, O., Tsai, M.Y., Speck, J.S.** Electron Transport Properties of Antimony Doped Sno_2 Single Crystalline Thin Films Grown by Plasma-assisted Molecular Beam Epitaxy *Journal of applied physics* 106 2009: pp. 093704.
https://doi.org/10.1063/1.3254241
28. **Syed, M.A., Syed, T.H., Shahzad, A.B., Jan, M., Rehman, N.U.** Effect of Doping on the Structural and Optical Properties of Sno_2 Thin Films Fabricated by Aerosol Assisted Chemical Vapor Deposition *6th Vacuum and Surface Sciences Conference of Asia and Australia (Vasscaa-6)* 439 2013: pp. 1 – 10.
https://dx.doi.org/10.1088/1742-6596/439/1/012013
29. **Xianjin, F., Luo, Y., Luan, C.** Effect of Annealing on the Structural and UV Photoluminescence Properties of Sb-doped Sno_2 Films Deposited on Al_2O_3 (0001) Substrates by RF Magnetron Sputtering *Optical Engineering* 53 (11) 2014: pp. 117111.
https://dx.doi.org/10.1117/1.OE.53.11.117111
30. **Mei-juan, L., Ping, C., Guo-qiang, L., Julie, M.S., Qiang, S.** Effects of Sb Oxidation State on the Densification and Electrical Properties of Antimony-doped Tin Oxide Ceramics *Journal of Materials Science: Materials in Electronics* 26 (6) 2015: pp. 4015 – 4020.
https://doi.org/10.1007/s10854-015-2938-y
31. **Yusheng, L., Jie, L., Jie, L., Xibin, Y., Li, D.** Tunable Solar-heat Shielding Property of Transparent Films Based on Mesoporous Sb-doped Sno_2 Microspheres *American Chemical Society Applied Materials & Interfaces* 7 (12) 2015: pp. 6574 – 6583.
https://doi.org/10.1021/am508711p
32. **Russameeruk, N., Naratip, V., Wanichaya, M., Jaran, S., Wisanu, P.** Sb-Doped SnO_2 Nanoparticles Synthesized by Sonochemical-Assisted Precipitation Process *Journal of Nanoscience and Nanotechnology* 15 (3) 2015: pp. 2564 – 2569.
https://doi.org/10.1166/jnn.2015.10222
33. **Raúl, B., Juan, M.S., Cesar, Q., Morallón, E.** Pt- and Ru-Doped SnO_2-Sb Anodes with High Stability in Alkaline Medium *American Chemical Society Applied Materials & Interfaces* 6 (24) 2014: pp. 22778 – 22789.
https://dx.doi.org/10.1021/am506958k
34. **Montero, J., Guillen, C., Herrero, J.** Discharge Power Dependence of Structural, Optical and Electrical Properties of DC Sputtered Antimony Doped Tin Oxide (ATO) Films *Solar Energy Materials & Solar Cells* 95 (8) 2011: pp. 2113 – 2119.
https://doi.org/10.1016/j.solmat.2011.03.009
35. **Sushil, K.P., Sushil, K.P., Vishnu, A., Shruti, V., Mukul, G., Mukherjee, S.** Spetroscopic Ellipsometry Study on Electrical and Elemental Properties of Sb-doped ZnO Thin Films *Current Applied Physics* 15 (4) 2015: pp. 479 – 485.
https://dx.doi.org/10.1016/j.cap.2015.02.008
36. **Gençyılmaz, O., Atay, F., Akyüz, I.** Deposition and Ellipsometric Characterization of Transparent Conductive Al-doped ZnO for Solar Cell Application *Journal of Clean Energy Technologies* 4 (2) 2016: pp. 90 – 94.
https://doi.org/10.7763/JOCET.2016.V4.259
37. **Saliha, E., Sadan, K., Pat, S.** Optical Characterization of Deposited ITO Thin Films on Glass and PET Substrates *Applied Surface Science* 276 2013: pp. 641 – 645.
https://dx.doi.org/10.1016/j.apsusc.2013.03.146
38. **Jiao, Y., Yiling, J., Linjie, L., Meizhen, G.** Structural, Morphological, Optical and Electrical Properties of Ga-doped Zno Transparent Conducting Thin Films *Applied Surface Science* 421 2017: pp. 446 – 452.
https://dx.doi.org/10.1016/j.apsusc.2016.10.079
39. **Atay, F., Bilgin, V., Akyuz, I., Ketenci, E., Kose, S.** Optical Characterization of Sno_2:F Films by Spectroscopic Ellipsometry *Journal of Non-Crystalline Solids* 356 (41 – 42) 2010: pp. 2192 – 2197.
https://doi.org/10.1016/j.jnoncrysol.2010.07.007
40. **Al-Douri, A.A.J., Alias, F.A., Alnajjar, A.A., Makadsi, M.N.** Electrical and Optical Properties of Ge_xSi_{1-x}:H Thin Films Prepared by Thermal Evaporation Method *Advances in Condensed Matter Physics* 2010: pp. 428739.
https://doi.org/10.1155/2010/428739
41. **Vazquez-Arreguın, R., Aguilar-Frutis, M., Falcony-Guajardo, C., Castaneda-Galvan, A., Mariscal-Becerra, L., Gallardo-Hernandez, S., Alarcon-Flores, G., Garcıa-Rocha, M.** Electrical, Optical and Structural Properties of SnO_2:Sb:F Thin Films Deposited from $Sn(acac)_2$ by Spray Pyrolysis *Electrochemical Society Journal of Solid State Science and Technology* 5 (3) 2016: pp. 101 – 107.
https://doi.org/10.1149/2.0211603jss
42. **Xiaotao, H., Jin, M., Deheng, Z., Yingge, Y., Xianggang, X., Feng, C., Ma, H.** Electrical and Optical Properties of SnO_2:Sb Films Prepared on Polyimide Substrate by r.f Bias Sputtering *Applied Surface Science* 891 (1 – 2) 2002: pp. 157 – 161.
https://doi.org/10.1016/S0169-4332(02)00014-4